ORIGINAL RESEARCH PAPER

Comparison of acute responses of mice livers to short-term exposure to nano-sized or micro-sized silver particles

Kyungeun Cha · Hye-Won Hong · Yeon-Gil Choi · Min Joo Lee · Jong Hoon Park · Hee-Kwon Chae · Gyuha Ryu · Heejoon Myung

Abstract Mice were fed either 13 nm silver nanoparticles or 2–3.5 μm silver microparticles. The livers were then obtained after 3 days and subjected to a histopathological analysis. The nanoparticle-fed and microparticle-fed livers both exhibited lymphocyte infiltration in the histopathological analysis, suggesting the induction of inflammation. In vitro, a human hepatoma cell line (Huh-7) was treated with the same silver nanoparticles and microparticles. The mitochondrial activity and glutathione production were hardly affected. However, the DNA contents decreased 15% in the nanoparticle-treated cells and 10% in the microparticle-treated cell, suggesting a more potent induction of apoptosis by the nanoparticles. From a microarray analysis of the RNA from the livers of the nano- and micro-particle-fed mice, the expression of genes related to apoptosis and inflammation was found to be altered. These gene expression changes in the nanoparticle-treated livers lead to phenotypical changes, reflecting increased apoptosis and inflammation. The changes in the gene expression were confirmed by using a semi-quantitative RT-PCR.

K. Cha · H.-W. Hong · Y.-G. Choi · H. Myung (✉)
Department of Bioscience and Biotechnology,
Hankuk University of Foreign Studies,
Yong-In, Kyung-Gi Do 449-791, Korea
e-mail: hjmyung@hufs.ac.kr

M. J. Lee · J. H. Park
Department of Biological Science, Sookmyung Women's
University, Seoul 140-742, Korea

H.-K. Chae
Department of Chemistry Education, Seoul National
University, Seoul 151-748, Korea

G. Ryu
Korea Food and Drug Administration,
Seoul 122-704, Korea

Introduction

Nano-sized materials are now being used in medicine, biotechnology, production lines, energy, and environmental technology. Nanotubes, nanowires, fullerene derivatives, quantum dots are examples of such nano materials being used for various applications (Bruchez et al. 1998; Cui et al. 2001; Husein et al. 2005; Taton et al. 2000). Nanoparticles have a higher surface to volume ratio compared to larger particles, which increases the chances of the atoms' localizing on the surface rather than inside and gives them unique physical properties. Sometimes nanoparticles are unstable and react with other materials in the vicinity, resulting in changed characteristics (Husein et al. 2005; Colvin 2003; Oberdorster 2004). For example, gold nanoparicles are red when they are smaller than 20 nm, while silver nanoparticles are yellow at a nano size. In addition to the physical changes, chemical

changes also occur. For example, nano-sized gold particles exhibit catalytic activity while nano-sized silver particles have an anti-bacterial effect.

Recent advances in nano-technology have increased the chances of contact between human and nano-sized materials. However, despite this increased exposure to nanoparticles, little information is available regarding the toxicity of nanoparticles toward animals including humans. Accordingly, to compare the effects caused by nano- and micro-sized silver particles, this study fed silver nanoparticles or microparticles to mice and compared the acute responses. In particular, the effects on the liver were examined since up to 50% of drug metabolism occurs in the liver.

Materials and methods

Mice feeding and histopathological observation

Seven-week-old male balb/c mice were starved for 24 h before being fed 2.5 g of nano- or micro-sized silver particles directly to the stomach. The livers were then taken after 3 days and fixed in 10% (v/v) formalin. Following 5 μm-thick sectioning, samples were mounted on glass slides and examined under a light microscope after hematoxylin-eosin staining (Green Cross, Korea).

Cell culture

A human liver cell line (Huh-7) was grown in Dulbecco's modified Earle's medium (DMEM) containing 1% antibiotics and 10% (v/v) fetal bovine serum (FBS) at 37°C in a 5% (v/v) CO_2 incubator.

Silver particles

Aldrich grade $AgNO_3$ and $NaBH_4$ (2×10^{-3} M) were used without further purification. A silver nanoparticle solution was prepared based on the reduction of $AgNO_3$ with $NaBH_4$ as described previously (Suh et al. 1983). Briefly, 60 ml $NaBH_4$ (2×10^{-3} M) was mixed with 22 ml $AgNO_3$ (1×10^{-3} M) under ice-cooled conditions. The resulting yellow solution was stirred for ∼1 h whenever the dark color appeared. The typical size of a colloid particle in the solution was about 13 nm, was characterized by TEM, and the maximum absorption was near 390 nm.

Mitochondrial activity

A MTT assay was used to measure the mitochondrial activity. The cells were seeded in a 96-well plate at 2.5×10^3 cells/well and incubated for 24 h before adding nanoparticles to each well at different concentrations and incubating the cells for a further incubated for 72 h. Next 10 μl 5 mg MTT/ml was added to each well and the cells were incubated for 3 h. After discarding the media, 50 μl DMSO was added to each well, the mixtures incubated for 10 min at 60°C, and the absorbance measured at 595 nm using a microplate reader.

DNA contents

The cells were seeded in a 24-well plate at 5×10^4 cells/well and incubated for 24 h before adding nanoparticles to each well at different concentrations and incubating the cells for a further 72 h. Next, the cells were washed once with phosphate buffered saline (PBS, pH 7.4), then 200 μl RIPA buffer (50 mM Tris, 1% NP-40, 0.5% sodium deoxycholate, 0.1% SDS, 150 mM NaCl) was added to each well and the cells incubated on ice for 30 min. Thereafter, the cultures were subjected to a centrifugation at $14,000 \times g$ for 10 min and 2 μl each lysed extract added to wells containing 100 μl bisbenzimide H 33258 solution (Sigma) (2 μg/ml) in a 96-well plate. Finally, the fluorescence was measured using a fluorometer at an excitation wavelength of 360 nm and emission wavelength of 460 nm.

Glutathione production

The cells were seeded in a 24-well plate at 5×10^4 cells/well and incubated for 24 h before adding nanoparticles to each well at various concentrations and incubating the cells for a further 72 h. After washing each well with PBS, the cells were subjected to homogenization with 5% (w/v) sulfosalicyclic acid, and the resulting homogenates centrifuged at $14,000 \times g$ for 5 min. 15 μl 100U glutathione reductase/ml (Sigma), 100 μl NADPH, and 15 μl DTNB were added to each homogenate and incubated at 37°C. Finally, the absorbance of each reactant was measured using a microplate reader at 412 nm.

Microarray analysis

The RNA was isolated from the livers of the nano-silver-particle-fed mice (see "Histopathological observation" section) using a total RNA isolation kit (Qiagen, USA). Reference RNA was also isolated from the livers of micro-silver-particle-fed mice using the same kit. The expression profiles were analyzed using an Agilent Whole Mouse Genome 44 K 4plex chip, and the service provided by Digital Genomics, Korea.

RT-PCR

One micro gram of the RNA isolated from the silver-particle-fed livers was subjected to annealing with an appropriate reverse transcription primer. dNTPs and reverse transcriptase (Invitrogen, USA) were added to synthesize first strand cDNA, after which Taq polymerase (Solgent, USA), appropriate primers, and dNTPs were added for a PCR reaction to produce double strand cDNA products. The glyceraldehydes-3-dehydrogenase gene was used as the control. For semi-quantitative purposes, the number of polymerization cycles was adjusted between 15 and 25 according to the expression level of each gene.

PathwayStudio analysis

PathwayStudio builds pathways using various methods. This software has a built-in resource called ResNet, which is a database for searching molecular interactions through natural language processing of scientific abstracts contained in the PubMed database. From ResNet, we were able to add our interesting gene product onto a new pathway diagram and build a new pathway based on well-known interactions referred to in the relevant literature.

Results

In vitro cytotoxic response

The effect of silver nanoparticles (see Fig. 1) on the energy metabolism of liver cells was measured. Almost no reduction in mitochondrial activity reduction was seen in the livers from the mice fed with nano- or micro-sized particles (Fig. 2a). Conversely,
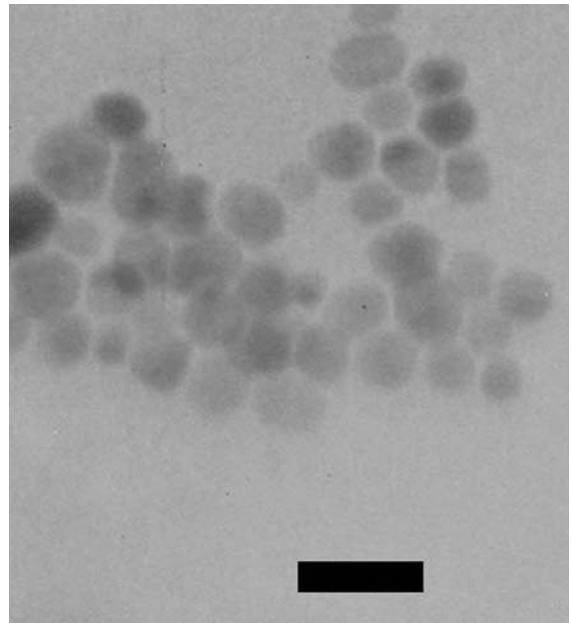

Fig. 1 13 nm silver nanoparticles used in this study. Bar represents 20 nm

the DNA contents were decreased up to 18% in the nanoparticle-fed livers and up to 10% in the micro-particle-fed livers (Fig. 2b). Yet no dose-dependency was observed in the nanoparticle-fed samples and only a weak dose-dependency observed in the microparticle-fed samples. Glutathione is a natural antioxidant and produced when a cell is under oxidative stress. However, when checking the glutathione production to test for oxidative stress, there was hardly any change in the glutathione production with the nano- or micro-silver particles (Fig. 2c).

Histopathological observation

Focal lymphocyte infiltration was observed in both the nano- and micro-size particle-fed liver portal tracts (Fig. 3), suggesting the induction of inflammation. Plus, in the case of the nanoparticle-fed mice, nonspecific focal hemorrhages were observed in the heart, focal lymphocyte infiltration observed in the intestine, and nonspecific medullary congestion observed in the spleen (data not shown).

Changes in gene expression profile

In the case of the genes involved in apoptosis, three genes (coding for cyclin-dependent kinase inhibitor
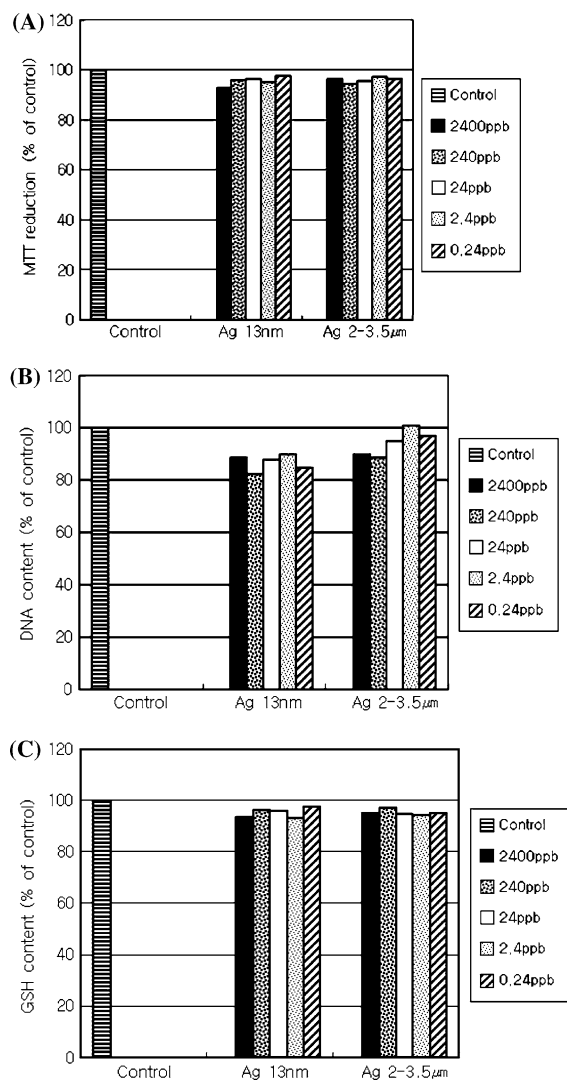
Fig. 2 Comparison of cytotoxic effects induced by nano- and micro-sized silver particles. (**a**) Measurement of mitochondrial activity using MTT assay of liver cells from mice fed either nano- or micro-sized silver particles. (**b**) Measurement of DNA content in liver cells from mice fed either nano- or micro-sized silver particles. (**c**) Measurement of glutathione production in liver cells from mice fed either nano- or micro-sized silver particles

Fig. 3 Hematoxylene-eosin staining of liver tissue from mice fed nano- or micro-sized silver particles. Magnification was 400×. (**a**) Liver tissue from mice fed nano-sized silver particles. (**b**) Liver tissue from mice fed micro-sized silver particles

1A, α-synuclein, and Bcl-2 modifying factor) were upregulated 3.1- to 6.4-fold, while 4 genes (coding for chemokine ligand 1, heat-shock 70 kDa protein 2, interleukin 7, and ATP-binding cassette, subfamily B) were significantly downregulated in the livers treated with nanoparticles when compared to the livers treated with microparticles (Table 1). Similarly, in the case of genes involved in inflammation, certain genes (coding for keratin 16, chemokine ligand 13, and a macrophage
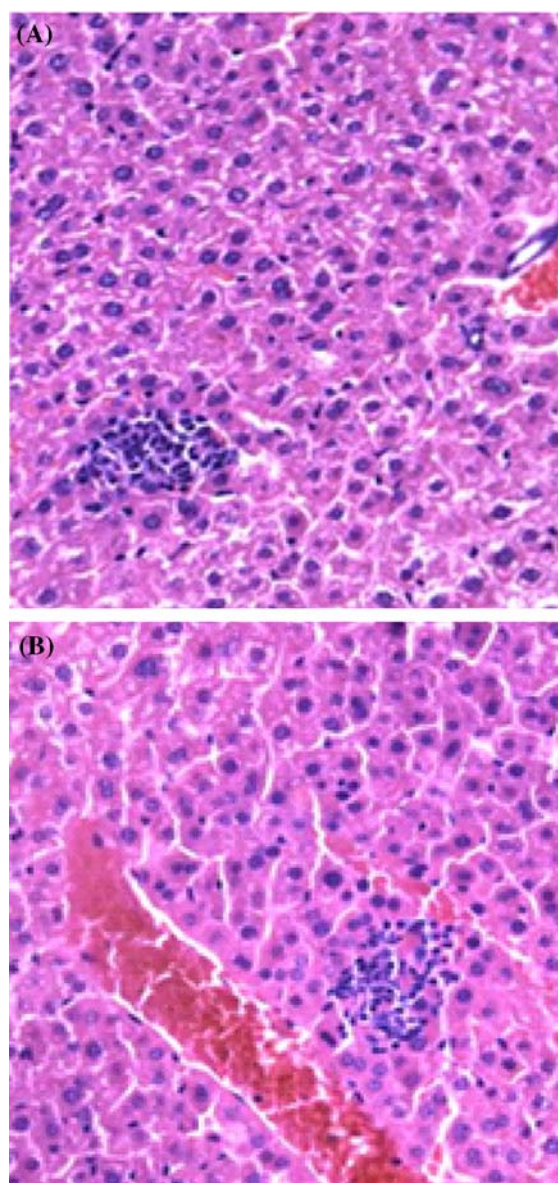
receptor with a collagenous structure) were upregulated 3.1- to 3.2-fold, while other genes (coding for nuclear receptor subfamily 1, group D, and chemokine ligand 7) were significantly downregulated in the livers treated with nanoparticles. These changes in the expression of selected genes were confirmed by a semi-quantitative RT-PCR (Fig. 4). Based on the

Table 1 Genes related to apoptosis and inflammation showing expression changes

Function	Genbank accession number	Name	Fold change
Apoptosis	NM_007669	Cyclin-dependent kinase inhibitor 1A	6.35
	NM_009221	Synuclein, alpha	3.58
	NM_138313	Bcl2 modifying factor	3.11
	NM_008176	Chemokine (C-X-C motif) ligand 1	0.32
	NM_008301	Heat shock 70 kDa protein 2	0.27
	NM_008371	Interleukin 7	0.25
	NM_011075	ATP-binding cassette, sub-family B (MDR/TAP)	0.19
Inflammation	NM_008470	Keratin 16	3.92
	NM_018866	Chemokine (C-X-C motif) Ligand 13	3.11
	NM_010766	Macrophage receptor with collagenous structure	3.11
	NM_011584	Nuclear receptor subfamily 1, group D, member 2	0.22
	NM_023785	Chemokine (C-X-C motif) ligand 7	0.16

expression profile changes in response to the treatments with nanoparticles or microparticles, possible pathways for apoptosis and inflammation were obtained (Fig. 5).

Discussion

As the use of nanoparticles in various applications continues to increase, concern about their potential toxicity is also growing. Most nanoparticles in use today have existed as microparticles in nature for a long time. Thus, the toxicity related to such micro-sized particles is already known. Therefore, the purpose of this study was to compare the effects induced by nano- and micro-sized silver particles.

In vitro, the cultured cells hardly showed any change in their survival in MTT assay or glutathione production with both-sizes of particles, meaning the mitochondrial activity and oxidative stress were minimal. However, a greater decrease in the DNA contents was observed in the nanoparticle-treated cells, suggesting the induction of a higher level of apoptosis. Plus, when analyzing the livers from nano- and microparticle-fed mice, both showed signs of inflammation, although a higher degree was observed in the nanoparticle-fed mice.

Therefore, the above findings prompted an in vivo examination of the changes in the gene expression profile for the nano- and microparticle-treated liver cells. As expected, the expression of genes related to apoptosis and inflammation was altered when
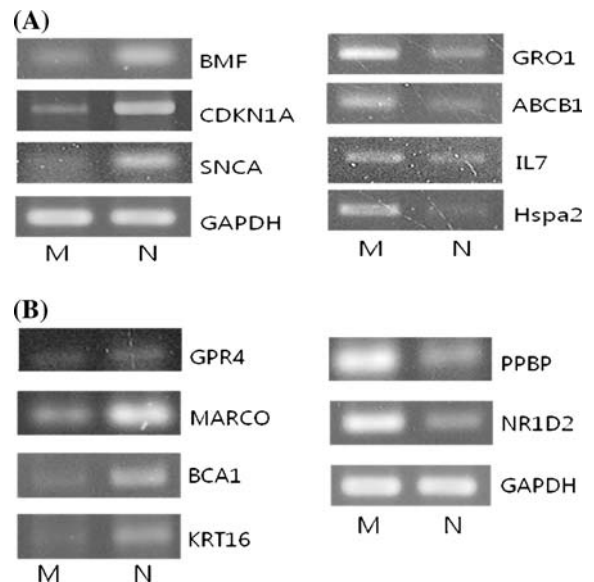

Fig. 4 Confirmation of expression change of genes related to apoptosis and inflammation. Expression levels were checked using semi-quantitative RT-PCR. GAPDH was used as internal control. M, Genes from microsized silver particle-fed mice livers; N, Genes from nano-sized silver particle-fed mice livers. (**a**) Genes related to apoptosis. (**b**) Genes related to inflammation

comparing the liver cells. PathwayStudio built several pathways from the gene lists provided by the authors and found paths among molecules/cell objects/processes. The algorithm used to reconstruct the signaling pathways is described, and was validated based on comparison with manually created pathways and gene-specific expression profiles. Based on the gene
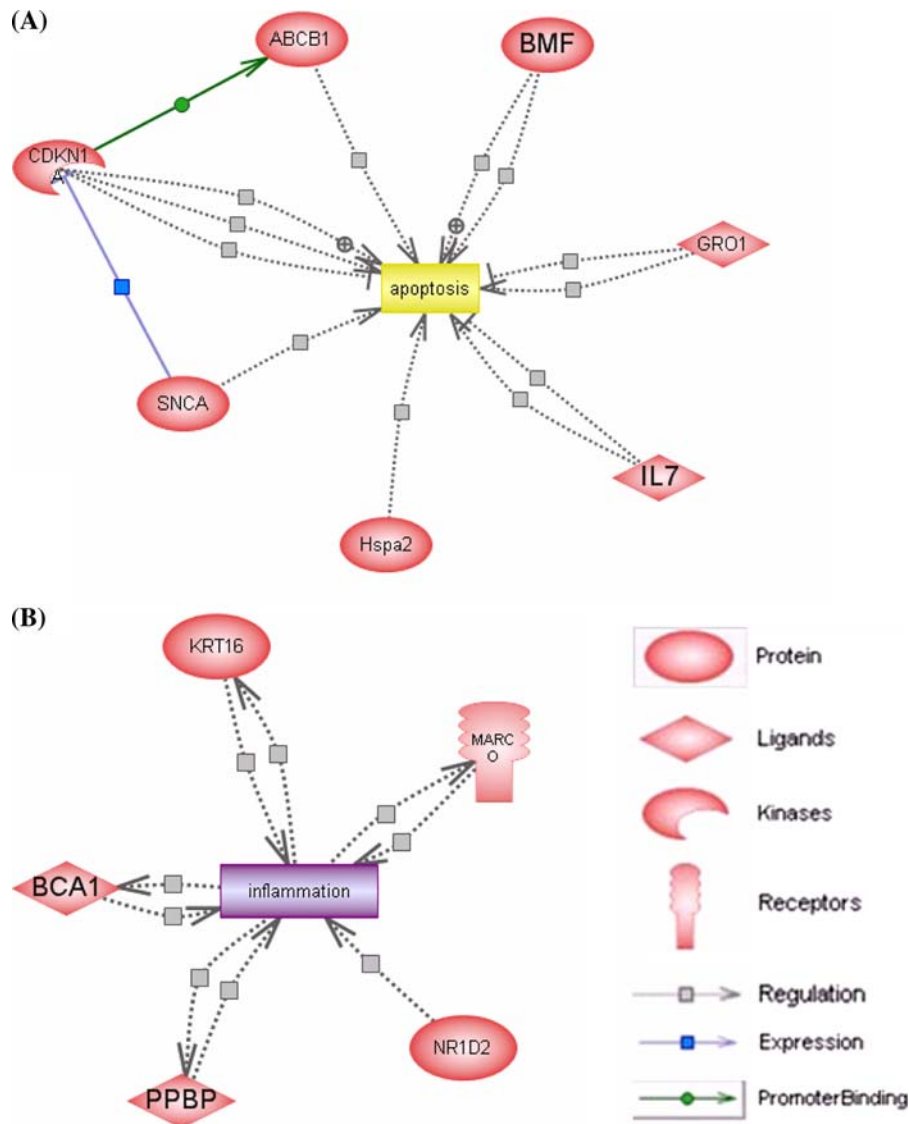
Fig. 5 Manually built pathway of genes related to apoptosis and inflammation. (**a**) Apoptosis, (**b**) inflammation

expression profiles in Table 1, all possible pathways for apoptosis and inflammation were obtained. In Fig. 4, each color and symbol in the interaction between proteins is informative in terms of the relationships of apoptosis and inflammation.

Cyclin dependent kinase inhibitor 1A (p21) is activated by p53 (Child and Mann 2006). α-Synuclein causes derangements in vesicle processing, including protein turnover, mitochondrial function, and oxidative stress, the occurrence of which have all been suggested to lead to apoptosis (Cookson and van der Brug 2008). Bcl-2 is a pro- and anti-apoptotic protein

related to cytochrome c release (Schultz and Harrington 2003). Thus the elevated expression of these three genes can lead to increased apoptosis. Meanwhile, chemokine ligand 1 has been reported to be involved in an anti-apoptotic pathway (Louahed et al. 2003). Heat-shock 70 kDa protein 2 is expressed in response to a wide variety of physiological and environmental insults including anticancer chemotherapy, to help the cell to survive under lethal conditions meaning it exhibits anti-apoptotic activity (Garrido et al. 2006). Interleukin 7 is known to be produced from human hepatocytes (Rowell et al.

1997) and induces a Bcl-2 response (Hofmeister et al. 1999). The ATP-binding cassette, subfamily B (MDR/TAP) is a member of ABC proteins and is known to be related to apoptosis (Klein et al. 1999). Thus the downregulation of these four genes can also lead to increased apoptosis.

Keratin 16 is produced at a higher level in inflammatory responses including psoriasis (Lew et al. 2004). Chemokine ligand 13 is related to the selective recruitment of mononuclear and granulocytic cells, leading to inflammation. (Mendez-Enriquez et al. 2008). A macrophage receptor with a collagenous structure (MARCO) is known to be expressed from the microbial stimulation of immune activation. (Mukhopadhyay et al. 2004). Thus the upregulation of these three genes can lead to increased inflammation. Meanwhile nuclear receptor subfamily 1, group D, works in monocyte/macrophages, where the ligands of this receptor partly inhibit the activation of macrophages and the production of inflammatory cytokines (TNF alpha, interleukin 6 and 1beta) (Cabrero et al. 2002). The non-glycosaminoglycan (GAG)-binding pleiotropic chemokine CCL7 has been reported to antagonize chemokine-mediated inflammation (Ali et al. 2005). Thus, the downregulation of these two genes could lead to increased inflammation.

In conclusion, clear differences were found in gene expression, especially in relation to apoptosis and inflammation, when comparing the liver cells liver cells exposed to nano- and micro-sized silver particles in vivo. Thus further studies are needed to elucidate the underlying mechanisms.

References

Ali S, Robertson H, Wain JH, Isaacs JD, Malik G, Kirby JA (2005) A non-glycosaminoglycan-binding variant of CC chemokine ligand 7 (monocyte chemoattractant protein-3) antagonizes chemokine-mediated inflammation. J Immunol 175:1257–1266

Bruchez M, Moronne M, Gin P, Weiss S, Alivisatos AP (1998) Semiconductor nanocrystals as fluorescent biological labels. Science 281:2013–2016

Cabrero A, Laguna JC, Vázquez M (2002) Peroxisome proliferator-activated receptors and the control of inflammation. Curr Drug Targets Inflamm Allergy 1:243–248

Child ES, Mann DJ (2006) The intricacies of p21 phosphorylation: protein/protein interactions, subcellular localization and stability. Cell Cycle 5:1313–1319

Colvin V (2003) The potential environmental impacts of engineered nanomaterials. Nat Biotechnol 21:1166–1170

Cookson MR, van der Brug M (2008) Cell systems and the toxic mechanism(s) of alpha-synuclein. Exp Neurol 209:5–11

Cui Y, Wei Q, Park H, Lieber C (2001) Nanowire nanosensors for highly sensitive and selective detection of biological and chemical species. Science 293:1289–1292

Garrido C, Brunet M, Didelot C, Zermati Y, Schmitt E, Kroemer G (2006) Heat shock proteins 27 and 70: anti-apoptotic proteins with tumorigenic properties. Cell Cycle 5:2092–2601

Hofmeister R, Khaled AR, Benbernou N, Rajnavolgyi E, Muegge K, Durum SK (1999) Interleukin-7: physiological roles and mechanisms of action. Cytokine Growth Factor Rev 10:41–60

Husein S, Hess K, Gearheart J, Geiss K, Schlager J (2005) In vitro toxicity of nanoparticles in BRL 3A rat liver cells. Toxicol In Vitro 19:975–983

Klein I, Sarkadi B, Váradi A (1999) An inventory of the human ABC proteins. Biochim Biophys Acta 1461:237–262

Lew W, Lee E, Krueger JG (2004) Psoriasis genomics: analysis of proinflammatory (type 1) gene expression in large plaque (Western) and small plaque (Asian) psoriasis vulgaris. Br J Dermatol 150:668–676

Louahed J, Struyf S, Demoulin JB, Parmentier M, Van Snick J, Van Damme J, Renauld JC (2003) CCR8-dependent activation of the RAS/MAPK pathway mediates anti-apoptotic activity of I-309/CCL1 and vMIP-I. Eur J Immunol 33:494–501

Mendez-Enriquez E, Melendez Y, Martinez F, Baay G, Huerta-Yepez S, Gonzalez-Bonilla C, Fortoul TI, Soldevila G, García-Zepeda EA (2008) CDIP-2, a synthetic peptide derived from chemokine (C–C motif) ligand 13 (CCL13), ameliorates allergic airway inflammation. Clin Exp Immunol [Epub ahead of print]

Mukhopadhyay S, Peiser L, Gordon S (2004) Activation of murine macrophages by Neisseria meningitidis and IFN-gamma in vitro: distinct roles of class A scavenger and toll-like pattern recognition receptors in selective modulation of surface phenotype. J Leukoc Biol 76:577–584

Oberdorster E (2004) Manufactured nanomaterials (fullerenes, C60) induce oxidative stress in the brain of juvenile largemouth bass. Environ Health Perspect 112:1058–1062

Rowell DL, Eckmann L, Dwinell MB, Carpenter SP, Raucy JL, Yang SK, Kagnoff MF (1997) Human hepatocytes express an array of proinflammatory cytokines after agonist stimulation or bacterial invasion. Am J Physiol 273:G322–G332

Schultz DR, Harrington WJ Jr (2003) Apoptosis: programmed cell death at a molecular level. Semin Arthritis Rheum 32:345–369

Suh JS, DiLella DP, Moskovits M (1983) Surface-enhanced Raman spectroscopy of colloidal metal systems. J Phys Chem 87:1540–1544

Taton T, Mirkin C, Letsinger R (2000) Scanometric DNA array detection with nanoparticle probes. Science 289:1757–1760